Dalton Transactions

ROYAL SOCIETY OF CHEMISTRY

PAPER

View Article Online
View Journal

Cite this: DOI: 10.1039/d4dt01663g

Stoichiometry effect on the structure, coordination and anticancer activity of gold(I/III) bisphosphine complexes†

Adedamola S. Arojojoye, [a] Justin Holmes,[a] Oluwatosin A. Obisesan,[a] Sean Parkin [a] and Samuel G. Awuah *[a,b,c]

Rationalizing the impact of oxidation states of Au-based complexes on function require synthetic strategies that allow for conserved molecular formula in Au(I) and their Au(III) counterparts. Oftentimes achieving Au(I) and Au(III) coordination complexes with the same ligand system is challenging due to the reactivity and stability of the starting Au(I) or Au(III) starting materials. Thus, attempts to study the impact of oxidation state on biological function has been elusive. We posit that Au complexes with the same ligand framework but different oxidation states will affect complex geometry and hence elicit differences in biological function or mechanism. In this work, we reacted 1,2-bis(diphenylphosphino)benzene with respective Au starting materials in different mole ratios to facilitate the synthesis of structurally distinct Au(I) or Au(III) complexes. Briefly, by reacting two stoichiometric equivalents of $HAuCl_4{\cdot}3H_2O$ or $AuCl_3$(tht) with one equivalent of 1,2-bis(diphenylphosphino)benzene, we obtained dicationic bis-[1,2-bis-(diphenylphosphino)benzene]gold(III) chloride whereas an equimolar ratio of $HAuCl_4{\cdot}3H_2O$ and 1,2-bis(diphenylphosphino)benzene gave the monocationic bis-[1,2-bis-(diphenylphosphino)benzene]gold(I) complex in moderate yield. The complexes were characterized spectroscopically by HRMS, RP-HPLC-MS, NMR and the purity ascertained by elemental analysis. The ^{31}P NMR showed characteristic singlet peak at ~22 ppm for the Au(I) complexes and ~57 ppm for the Au(III) complexes. The structure of the Au(III) complexes was further confirmed by X-ray crystallography as a 5-coordinate Au(III) complex. Although both Au(I) and Au(III) complexes showed promising anticancer activity in MDA-MB-231 (breast cancer) and BT-333 (glioblastoma) cancer cell lines and inhibited maximal mitochondria respiration in MDA-MB-231 cells, the Au(III) complexes further induce ROS accumulation and facilitate depolarization of the mitochondria membrane potential in MDA-MB-231 cells. Taken together, the synthetic approach provides a way to elucidate the effect of Au(I)/Au(III) oxidation states on structure, activity, and potential mechanism with respect to the same ligand.

Received 7th June 2024,
Accepted 4th December 2024

DOI: 10.1039/d4dt01663g

rsc.li/dalton

Introduction

Traditional first- and second-generation platinum drugs (cisplatin, carboplatin) remain the active chemotherapeutic drugs in the clinic,[1–3] but their lack of selectivity results in severe side effects, and drug resistance toward cancer cells has prompted research into alternative anticancer therapies.[4–10] Research into the use of Au complexes as therapeutic agents has seen immense development in the past two decades.[11–20] This is due to the distinct electronic properties and relativistic effect of Au at the atomic level compared to other transition metals, which make the chemistry of Au extremely fascinating.[21–24] Biologically useful Au complexes exist majorly in two oxidation states of +I or +III.[25,26] In the +I oxidation state, Au(I) complexes have a d^{10} electronic configuration, act as soft Lewis acids, and form linear, tricoordinate, distorted square planar or tetrahedral geometries with soft bases (ligands).[25,27] The Au(III) counterpart with d^8 outer electronic configuration acts as a borderline soft–hard acid and exists in the square planar geometry and the unusual distorted square pyramidal geometry.[25,27]

The choice of ligand coordinated to the Au central atom can determine its structure, geometry, rigidity, redox behavior, stability, and cytotoxicity.[28–31] Bidentate ligands such as diketonates, carbenes, DACH, dithiocarbamates, and diphosphines are examples of bidentate ligands employed in the synthesis of

[a]Department of Chemistry, University of Kentucky, Lexington, KY 40506, USA. E-mail: awuah@uky.edu
[b]Center for Pharmaceutical Research and Innovation and Department of Pharmaceutical Sciences, College of Pharmacy University of Kentucky, Lexington, KY 40536, USA
[c]Markey Cancer Centre, University of Kentucky, Lexington, KY, 50536, USA

†Electronic supplementary information (ESI) available: Experimental section, Table S1 and Fig. S1–S39. CCDC 2345565 and 2345566. For ESI and crystallographic data in CIF or other electronic format see DOI: https://doi.org/10.1039/d4dt01663g

Au-based complexes.[15,32,33] The use of phosphine ligands as chelates in Au(I/III) complexes has gained more prominence since the approval of auranofin as an anti-arthritis drug by FDA and subsequent clinical trials for its repurposing in other diseased conditions. Despite the perceived innocence of phosphine ligands in metal-based reactions, they tend to tune the steric and electronic properties of the metal center for stability resulting in unprecedented biological activity of the metal complex distinct from the metal or ligand alone.[34]

The 1,2-bis(diphenylphosphino)benzene (DPPBz) ligand is a bidentate diphosphine ligand commonly used in coordination and organometallic chemistry with varied applications.[35] In catalysis, DPPBz was used in polyfluoroarylation of primary and secondary alkyl halides, where it facilitates the selective cleavage of Csp^3–halogen in an iron-catalyzed cross coupling reaction.[36] Cu complexes of 1,2-bis(diphenylphosphino)benzene has also been used in β-boration of α,β-unsaturated amide,[37] and *N*-formylation of a wide range of amines.[38] Zerovalent Ni-DPPBz complexes have also been used in the synthesis of alkoxysilanes by either the catalytic hydrosilylation of benzaldehyde by $PhSiH_3$ and Ph_2SiH_2, or the dehydrocoupling of benzyl alcohol by $PhSiH_3$ and Ph_2SiH_2.[39] In organic materials, DPPBz ligands has been used to synthesize materials with high luminescence performance for light emitting diodes, bioimaging, chemosensing and photoswitches.[40–43] In biology, 1,2-bis(diphenylphosphino) benzene has been used to synthesize metal complexes with anticancer,[44–47] and antimicrobial properties.[48,49] Our lab has also contributed to the synthesis of Au-DPPBz compounds that has revealed structural insights leading to new classes of organogold reagents with distinct biological applications. Earlier, we developed linear and distorted square planar Au(I) DPPBz complexes that showed activities against a panel of fungal strains. The complexes displayed potency against strains of *C. albicans* and *C. neoformans* with minimum inhibitory concentration (MIC) between 0.12–7.8 μg mL^{-1} in the fungal strains studied.[49] Furthermore, our lab developed cyclometalated Au(III) DPPBz compounds with either C^C or C^N cyclometalated systems.[47,50] The C^C cyclometalated Au(III) DPPBz compound showed great biological stability when reacted with L-glutathione, displayed potent anticancer activity in a broad spectrum of cancer cell lines and depolarized mitochondria membrane in isolated mitochondria of mouse liver.[47] The Au(III) DPPBz C^N compounds interact with mitochondria functions thereby providing therapeutic options in cancer treatment, chronic colitis and correcting metabolic dysfunction in inflammatory bowel disease.[50–52]

In this work, we report on the synthesis of novel Au(I) and Au(III) complexes bearing 1,2-bis(diphenylphosphino)benzene ligands for an unbiased characterization of the impact of oxidation state on antiproliferative activity in cells. The Au(III) complexes appear to have a unique structural scaffold with the central Au atom bonded to four (4) phosphorus atoms from DPPBz and coordination to a labile chlorine atom giving rise to complexes with a 5-coordinate geometry. The complexes reported showed anticancer activity in both triple negative breast cancer cell (MDA-MB-231) and human glioblastoma cell (BT-333) while inhibiting maximal respiration in MDA-MB-231 cancer cells. Furthermore, the Au(III) complexes induce ROS accumulation, depolarize mitochondria membrane potential, and showed improved cellular and mitochondria uptake compared to Au(I) complexes in MDA-MB-231 breast cancer cells.

Results

Synthesis and characterization of gold(I)/(III) complexes

Previous reports on the synthesis of Au(I) DPPBz complexes started with adding a THF solution of $Au(PPh_3)Cl$ to DPPBz, followed by addition of the appropriate salt in a second step.[43,53] We wanted to achieve the synthesis in one pot, therefore we employed the use of tetrachloroauric(III) acid trihydrate as the starting material. Briefly, the Au(I) complexes were synthesized in a single step by reacting an equimolar ratio of tetrachloroauric(III) acid trihydrate ($HAuCl_4{\cdot}3H_2O$) in dichloromethane with 1,2-bis(diphenylphosphino)benzene (DPPBz) in the presence of the appropriate sodium or potassium salt to afford four monocationic Au(I) DPPBz complexes with different counterions including **1-AuCl$_4$**, **1-Cl**, **1-BF$_4$** and **1-PF$_6$** (Fig. 1a). Tetrachloroauric acid ($HAuCl_4{\cdot}3H_2O$) is present in solution as H^+ and $AuCl_4^-$ ions. In the presence of bisphosphine ligands it is plausible that the [AuCl-DPPBz] intermediate forms. The ability for phosphine ligands to donate a lone pair of electrons to the d-shell of Au can facilitate the reduction and stabilization of the metal complex formed.

The novel Au(III) complexes were synthesized either by reacting 2 mol equivalence of tetrachloroauric(III) acid trihydrate ($HAuCl_4{\cdot}3H_2O$) with 1,2-bis(diphenylphosphino)benzene (DPPBz) in DCM to afford **3-AuCl$_4$** (Fig. 1b) or by reacting 2 mol equivalence of trichloro(tetrahydrothiophene)gold(III)

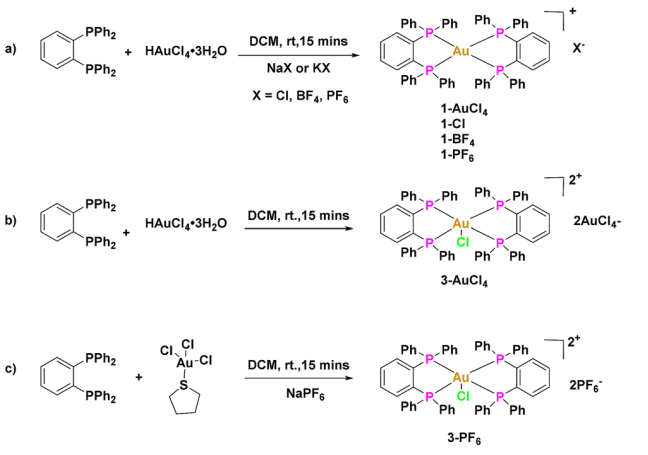

Fig. 1 Synthetic scheme showing the synthesis of Au(I/III) DPPBz complexes. (a) Synthesis of Au(I) complexes from equimolar ratio of ($HAuCl_4{\cdot}3H_2O$) and DPPBz with different counterions. (b and c) Synthesis of Au(III) complexes from either tetrachloroauric(III) acid trihydrate ($HAuCl_4{\cdot}3H_2O$) or trichloro(tetrahydrothiophene)gold(III) [$AuCl_3$(tht)].

$[AuCl_3(tht)]$ with 1,2-bis(diphenylphosphino)benzene (DPPBz) to afford **3-PF$_6$** (Fig. 1c). All complexes were characterized spectroscopically by ^{1}H, ^{31}P and ^{13}C NMR and purity accessed by RP-HPLC-MS (Fig. S2–27†). The ^{31}P NMR of the Au(I) complexes was 22 ppm similar to earlier published works.[43,49] For the Au(III) complex 3-AuCl$_4$, we observed a shift further downfield in the ^{31}P NMR at 57 ppm. Interestingly, when $NaPF_6$ salt was added to the reaction to facilitate exchange of counterion 3-PF$_6$ we observed a shift upfield in the ^{31}P NMR to about 29.9 ppm (Fig. S10†) indicating a possible reduction of the Au(III) center atom. Analysis of HPLC-MS results shows that P gets oxidized to P=O giving rise to an additional peak on the chromatogram and attendant *m*/*z* peak observed in the mass spectra.

Crystallography

Single crystals of **3-AuCl$_4$** and **3-PF$_6$** were grown by slow diffusion of ether into concentrated chloroform solution of **3-AuCl$_4$** and **3-PF$_6$** to further provide evidence for Au(III) compounds Fig. 2 and Fig. S1, Table S1.† **3-AuCl$_4$** crystallizes as a dicationic Au(III) complex with triclinic crystal system in *P*1 space group. The Au–Cl bond length is 2.7061 Å, while the Au–P bond length is Au1–P1 = 2.372 Å, Au1–P3 = 2.379 Å, Au1–P4 2.407 Å and Au1–P2 2.407 Å. The observed bond angles are P1–Au1–P3 175.34, P1–Au1–P4 97.62, P3–Au1–P4 81.08, P1–Au1–P2 80.94, P3–Au1–P2 99.55, P4–Au1–P2 169.76, P1–Au1–Cl1 95.79, P3–Au1–Cl1 88.79, P4–Au1–Cl1 94.89, P2–Au1–Cl1 95.34 indicating a square pyramidal geometry. **3-PF$_6$** crystallizes as a dicationic complex with mixed anion (PF_6 and Cl) in a monoclinic *C*2/*c* space group. The Au–Cl bond length is Au1–Cl 2.7087 Å, while the Au–P bond length is Au1–P2 = 2.3881, Au1–P2#1 = 2.3882, Au1–P1 = 2.3966, Au1–P1#1 = 2.3967. The observed bond angles P2–Au1–P2#1 = 172.87, P2–Au1–P1 = 80.567(16), P2#1–Au1–P1 = 99.153(16), P2–Au1–P1#1 = 99.154(16), P2#1–Au1–P1#1 = 80.572(16), P1–Au1–P1#1 = 175.61(2), P2–Au1–Cl1 = 93.565, P2#1–Au1–Cl1 = 93.565, P1–Au1–Cl1 = 92.196, P1#1–Au1–Cl1 = 92.196 indicating a square pyramidal geometry.

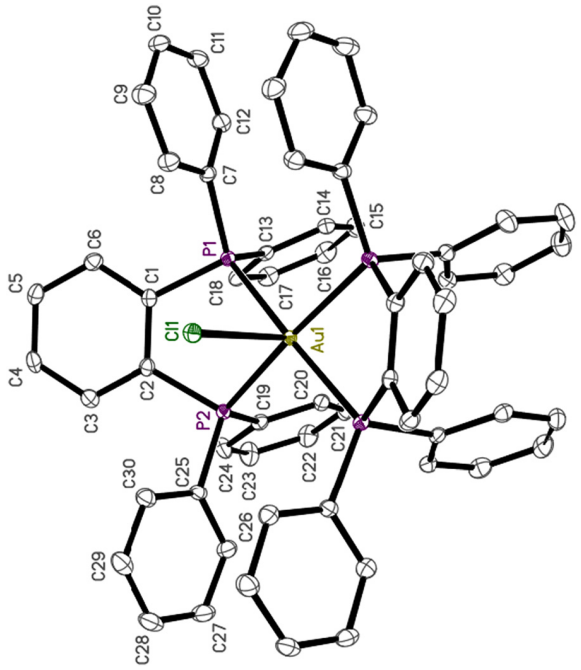

Fig. 2 Crystal structure of the cation of **3-PF$_6$**. Thermal ellipsoids are shown at the 50% probability level. Hydrogen and solvent molecules are omitted for clarity. Only one representative molecule from the asymmetric unit is shown.

In vitro antiproliferative activity studies

Au(III) bisphosphine complexes have been shown to elicit anticancer properties and with the spectroscopic and single X-ray crystal structures of these complexes showing Au compounds in two different oxidation states, we tested the effect of oxidation states as a function of antiproliferative activity in two cancer cell models. For scientific rigor, two cancer cells from different tissue origin, specifically, MDA-MB-231 (triple negative breast cancer cell) and BT-333 (glioblastoma) were used. These adherent cancer cell lines were treated with all compounds for 72 h at a 3-fold dilution with a starting concentration of 100 μM. All tested compounds showed cytotoxicity in both cell lines tested with IC_{50} in the low micromolar range (0.3–4.9 μM). As seen in Table 1 and Fig. S28–33,† the impact of oxidation state on cytotoxicity was not significantly differentiated from the IC_{50} values obtained. We found that complexes with PF_6 counter ion showed a significant difference in IC_{50} values between the Au(I) and Au(III) complexes in both cancer cell lines tested. The Au(I) complex, **1-PF$_6$** was found to be more cytotoxic than its Au(III) **3-PF$_6$** counterpart by about 4–16-fold. Furthermore, we tested the compounds in MRC5 (human lung fibroblast) to determine selectivity between normal cells and cancer cells Fig. S34.† Except for **1-AuCl$_4$**, we observed about 3–6-fold difference in the IC_{50} values of all the compounds which points towards the selectivity of the compounds towards cancerous cells.

Solution stability studies

Intrigued by the antiproliferative activity and spectroscopic analysis of these compounds, we examined the solution stability of **1-Cl** and **3-AuCl$_4$** in biological media Dulbecco's modified Eagle's medium (DMEM) Fig. 3a and b. We observed that **1-Cl** was stable in DMEM for 48 h without the formation of new adducts or reduction in peak intensity Fig. 3a while **3-AuCl$_4$** also showed solution stability for 48 h but significant reduction in peak intensity after 1 h of incubation Fig. 3b.

Table 1 Table showing IC_{50} values (μM) in MDA-MB-231 and BT-333 cancer cell lines. Data is represented as mean ± S.D (*n* = 6)

Compounds	MDA-MB-231	BT-333	MRC5
1-AuCl$_4$	1.78 ± 0.15	1.30 ± 0.04	0.93 ± 0.02
3-AuCl$_4$	1.52 ± 0.21	1.38 ± 0.23	4.47 ± 0.05
1-PF$_6$	0.30 ± 0.10	0.38 ± 0.02	1.91 ± 0.03
3-PF$_6$	4.92 ± 0.21	1.76 ± 0.12	—
1-Cl	1.14 ± 0.12	0.41 ± 0.20	1.35 ± 0.04
1-BF$_4$	0.82 ± 0.11	0.66 ± 0.02	—

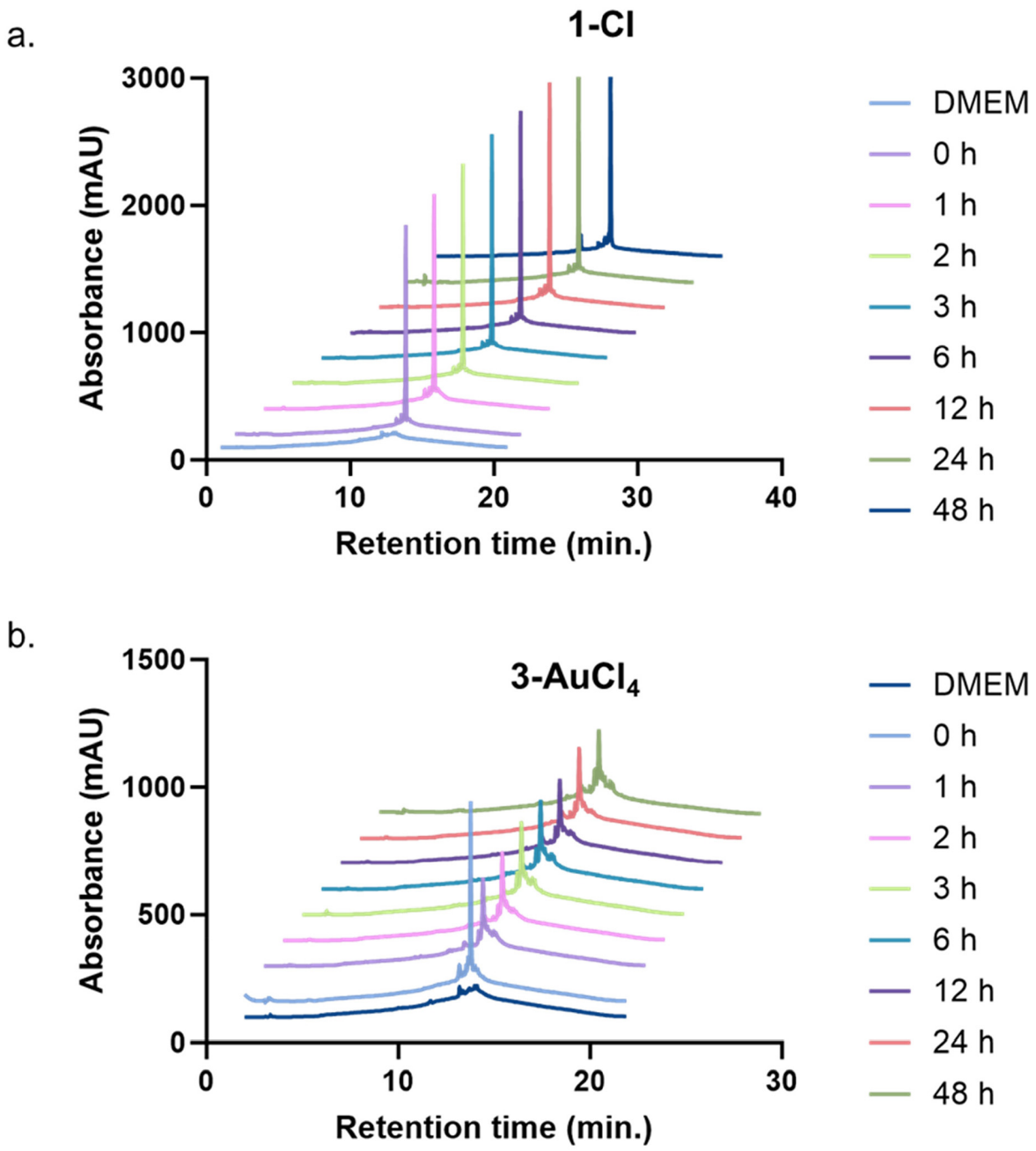

Fig. 3 Solution stability of (a) **1-Cl** and (b) **3-AuCl$_4$** in DMEM for 48 h. Reading was observed at λ = 260 nm.

Therefore, we proceeded with **1-Cl** and **3-AuCl$_4$** for further mechanistic studies.

Effects of oxidation state on cellular accumulation studies

Furthermore, we investigated the effect of the different oxidation states on metabolic function in cancer cells. Lipophilic cationic compounds accumulate in cells and organelles and the degree of charge on the compound can impact its uptake into cells. Therefore, we examined the role of oxidation state and hence the charge in a whole cell and isolated mitochondria setting in MDA-MB-231 cells. The intracellular accumulation when MDA-MB-231 cells were treated with compounds at 10 μM for 18 h was measured and we observed that Au(III) complexes **3-AuCl$_4$** and **3-PF$_6$** had a significantly higher whole cell uptake compared to their Au(I) counterparts. (Fig. 4a). Also, **1-Cl** and **1-PF$_6$** with chloride and PF_6 counterion was taken up more effectively compared to **1-AuCl$_4$** in MDA-MB-231 cancer cells highlighting the role counterions play in Au content uptake (Fig. 4a).

We therefore sought to examine the effect of oxidation state and charge on the uptake of these complexes in mitochondria. MDA-MB-231 (20 million) cells were treated with **1-Cl** and

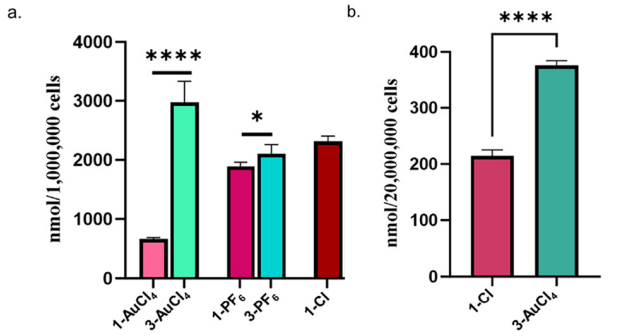

Fig. 4 Gold bioaccumulation studies. (a) Whole cellular uptake of Au(I/III) DPPBz complexes in MDA-MB-231 cancer cells. Cells were treated at a concentration of 10 μM for 18 h and Au concentration was determined by GFAAS. Data plotted as mean ± s.e.m (n = 3) (b) Mitochondria uptake of **1-Cl** and **3-AuCl$_4$** in MDA-MB-231 cancer cells. Cells were treated at a concentration of 10 μM for 18 h and Au concentration was determined by GFAAS. Data plotted as mean ± s.e.m (n = 2). Ordinary one-way ANOVA, *P < 0.05 **P < 0.01, ***P < 0.001, ****P < 0.0001. ns = not significant.

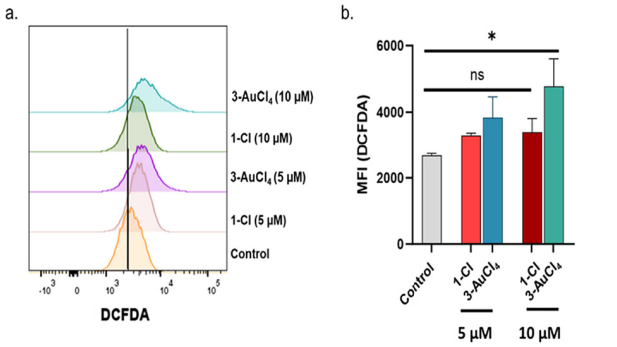

Fig. 5 ROS determination. (a) Histogram and (b) Bar chart showing MDA-MB-231 cells treated with **1-Cl** or **3-AuCl$_4$** at 5 and 10 μM for 2 h followed by staining with DCF-DA dye and the fluorescence intensity determined by flow cytometry at 488 nm. Ordinary one-way ANOVA *P < 0.05 **P < 0.01, ***P < 0.001, ****P < 0.0001. ns = not significant.

3-AuCl$_4$ at 10 μM for 18 h and subjected the treated cells to standard fractionation steps to obtain pure mitochondria. We observed that the more cationic Au(III) complex **3-AuCl$_4$** was significantly taken up into the mitochondria (375 nmol/20 million cells) compared to its Au(I) counterpart **1-Cl** (214.5 nmol/20 million cells) (Fig. 4b). These results suggest that the oxidation state, charge and the nature of counterion can dictate the bioavailability of a compound and should be taken into consideration in the design of anticancer Au compounds.

Effect of oxidation states on ROS

Next, we measured the intracellular ROS generated by **1-Cl** and **3-AuCl$_4$** to decipher how the oxidation state and charge relates to ROS production (Fig. 5). Using fluorescence-assisted cells sorting (FACS), MDA-MB-231 cells were treated with **1-Cl** or **3-AuCl$_4$** at 5 and 10 μM for 90 minutes and the cells were stained with 2′,7′-dichlorodihydrofluorescein diacetate fluorogenic dye and the amount of intracellular ROS accumulated was detected. We observed that at 10 μM there was a significant difference in the ROS produced by **3-AuCl$_4$** compared to **1-Cl** (Fig. 5a and b). This result suggests that the intracellular accumulation of reactive oxygen species (ROS) could be a contributor to cytotoxic activities observed for Au(III) DPPBz complexes in cancer cells.

Effect of 1-Cl and 3-AuCl$_4$ on mitochondria bioenergetics

We further studied the effect of oxidation states and charge of Au(I/III) complexes on mitochondria respiration (Fig. 6). **1-Cl** and **3-AuCl$_4$** were injected *via* a pneumatic injection which involves high pressured stream of fluid into MDA-MB-231 cancer cells, followed by different known inhibitors of the electron transport chain; oligomycin a complex V inhibitor, FCCP a protonophore that helps uncouple oxidative phosphorylation, antimycin/rotenone a complex I/III inhibitor. As seen in Fig. 6, we observed a concentration dependent inhibition of oxygen consumption rate (OCR) in maximal respiration for both compounds (Fig. 6a, b, d and e). For ATP linked respiration, only **3-AuCl$_4$** inhibited OCR in ATP linked respiration (Fig. 6c and f) pointing to a slight possibility of a different mechanism of cancer cell cytotoxicity. Taken together, the more cationic complex **3-AuCl$_4$** exhibited significant inhibition of maximal respiration and ATP respiration in MDA-MB-231 cancer cells compared to **1-Cl** (Fig. 6g and h).

Effect of 1-Cl and 3-AuCl$_4$ on mitochondria membrane potential

Decrease in ATP respiration may result from the loss of mitochondria membrane potential (MMP) and lead to changes in intermembrane space and matrix.[54] We examined the ability of these Au complexes to depolarize the mitochondria membrane potential by using a cationic lipophilic dye tetramethylrodamine ester (TMRE) that accumulates preferentially in active mitochondria giving rise to increased red fluorescence (high potential) while depolarized mitochondria shows a decrease in mitochondria membrane potential. Following the treatment of MDA-MB-231 cells with **1-Cl** and **3-AuCl$_4$** at 5 and 10 μM for 2 hours followed by staining with TMRE dye, we observed a concentration dependent decrease in fluorescence intensity of **3-AuCl$_4$** (about 53% at 10 μM) while **1-Cl** did not affect the mitochondria membrane potential significantly (Fig. 7). These results further affirm the difference in the mode of cancer cell cytotoxicity for both classes of complexes studied.

Discussion

The challenge of synthesizing Au(I) and Au(III) compounds with the same ligand framework can be overcome by changing the metal/ligand stoichiometric ratio. Previous work by Deng *et al.*, describing the effect of metal/ligand stoichiometry on the geometry and anticancer properties of Cu-based compounds showed that the stoichiometry did not affect the oxidation state of the Cu(II) complexes but significantly affected

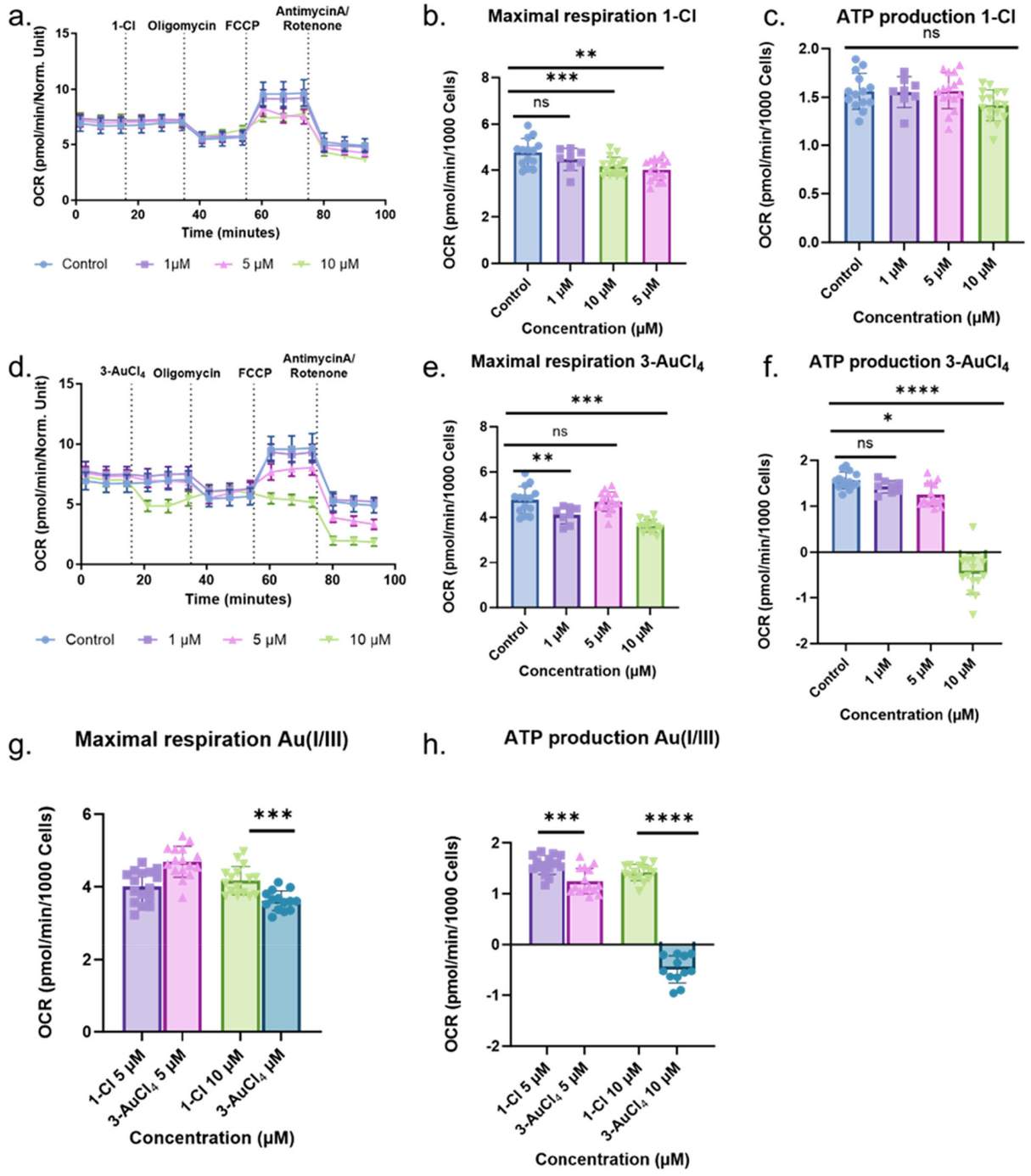

Fig. 6 Mitochondria bioenergetics study. (a) Seahorse assay of **1-Cl** administered *via* pneumatic injection *in vitro* to MDA-MB-231 plated cells followed by addition of various inhibitors of ETC at various time point. (b and c) Key parameters extrapolated from Seahorse assay of **1-Cl**. (d) Seahorse assay of **3-AuCl$_4$** administered *via* pneumatic injection *in vitro* to MDA-MB-231 plated cells followed by addition of various inhibitors of ETC at various time point. (e and f) Key parameters extrapolated from Seahorse assay of **3-AuCl$_4$**. (g and h) Effect of oxidation state on maximal respiration and ATP production. Ordinary one-way ANOVA,*P < 0.05 **P < 0.01, ***P < 0.001, ****P < 0.0001. ns = not significant.

the geometry and biological responses to cancer cells.[55] In this work, we report that change in the stoichiometric equivalence of Au/ligand can affect the oxidation state, geometry, and mechanism of anticancer activity. By rational design, the Au(I) and Au(III) complexes were synthesized efficiently without the need for purification by column chromatography except for **3-AuCl$_4$**. The synthetic strategy employed in the synthesis of the Au(III) complexes ensured the formation of Au(III) compound with unusual 5-coordinate geometry with the Au bonded to 4 phosphorus atoms and one chlorine atom. Cytotoxic phosphi-

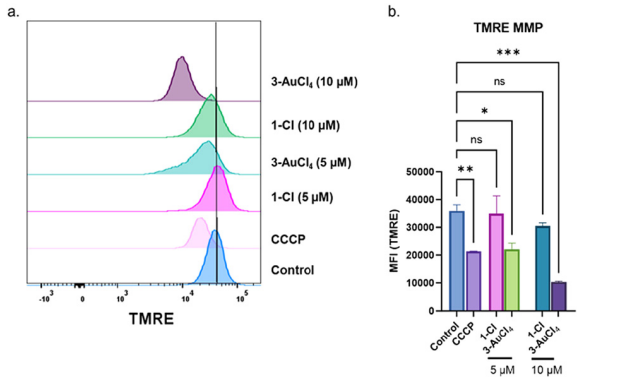

Fig. 7 MMP determination using TMRE dye. (a) Histogram and (b) Bar chart showing MDA-MB-231 cells treated with **1-Cl** or **3-AuCl$_4$** at 5 and 10 μM for 90 minutes and fluorescence observed by flow cytometry. Ordinary one-way ANOVA,*P < 0.05 **P < 0.01, ***P < 0.001, ****P < 0.0001. ns = not significant.

nogold(III) complexes with 5-coordinate geometry are rare in literature with few examples of complexes bearing N-donor ligands.[56–60] Moreover, the antiproliferative activity and mechanism of action studies for the Au(III) complexes aligns with previously reported Au(III) phosphine complexes in the literature. By inhibiting maximal respiration, ATP linked respiration, and depolarizing mitochondria membrane potential, these Au(III) cytotoxic compounds perturb the mitochondria dynamics in cancer cells where lipophilic cationic compounds tend to accumulate preferentially. We note here that other well-established putative targets of gold such as thioredoxin reductase is not ruled out as a potential target of these complexes. Whereas Au(III) reduction in cells is well-known, the high redox potential of Au(I)/(III) limit gold oxidation under physiological conditions. Unlike gold, Fe and Co by forming alkyl intermediates in enzymology can be oxidized. The ligands stabilizing the gold center may oxidize under aerobic conditions in cells.

Conclusions

In conclusion, we have reported the design of Au complexes bearing a DPPBz ligand in two different oxidation states but with the same cation molecular formula by selective synthetic reaction achieved *via* stoichiometry. Au(I) complexes are well known in the literature, and their biological activities and mechanism of action well studied in cancer cell model. For the novel Au(III) DPPBz complexes, we observed the unusual 5-coordinate Au(III) complex. The anticancer activity of the complexes in MDA-MB-231 and BT-333 cancer cells shows cytotoxicity in low micromolar range. Interestingly, while Au(I) complex (**1-Cl**) and its Au(III) counterpart shows inhibition of maximal respiration from 1 μM, only **3-AuCl$_4$** was able to inhibit ATP-linked respiration in MDA-MB-231 cells. Also, the MMP assay with TMRE showed that only the more cationic **3-AuCl$_4$** could depolarize the membrane potential significantly compared to **1-Cl**, indicating that the mechanism of cell death for both class of compounds is slightly different. Taken together, this work shows that changing the stoichiometric ratios of reactants can help to achieve the design of a vast library of Au complexes. Studies to further understand and exploit the 5-coordinate geometry of Au(III) complexes are currently ongoing.

Author contributions

Conceptualization, A. S. A. and S. G. A.; methodology, synthesis and characterization, biological assay A. S. A, J. H., and O. A. O.; X-ray crystallography S. P. writing original draft preparation, A. S. A.; writing review and editing, A. S. A. and S. G. A.; supervision, S. G. A.; funding acquisition, S. G. A.

Data availability

Data will be available to share upon request.

Conflicts of interest

The authors declare the following competing financial interest(s): S. G. A. has patents pending to the University of Kentucky Research Foundation.

Acknowledgements

This work and S. G. A. was supported by grant R01CA258421-01 from the National Cancer Institute. The authors would like to appreciate the following research centres and facilities at the University of Kentucky for their help towards the completion of the research described in this article. The UK NMR Center supported by NSF (CHE-997738) and the UK X-ray facility supported by the MRI program from NSF (CHE-1625732). We would like to thank Savita Sharma PhD for the support with our mitostress experiments, these experiments were carried out by support from the shared resource(s) of the University of Kentucky Markey Cancer Center (P30CA177558). The authors also acknowledge support of the Center for Pharmaceutical Research and Innovation (NIH P20GM130456). High resolution mass spectrometric analysis was performed at the University of Kentucky Mass Spectrometry and Proteomics Core facility and is supported in part by the Office of the Vice President for Research.

References

1 A. Kopacz-Bednarska and T. Król, *Oncol. Clin. Pract.*, 2022, **18**, 166–176.
2 I. Azar, O. Yazdanpanah, H. Jang, A. Austin, S. Kim, J. Chi, S. Alkassis, B. K. Saha, A. Chopra and K. Neu, *JAMA Network Open*, 2022, **5**, e2237699.

3 D. Tsvetkova and S. Ivanova, *Molecules*, 2022, **27**, 2466.
4 D. Cirri, L. Chiaverini, A. Pratesi and T. Marzo, *Comments Inorg. Chem.*, 2023, **43**, 465–478.
5 R. Ali, M. Aouida, A. Alhaj Sulaiman, S. Madhusudan and D. Ramotar, *Int. J. Mol. Sci.*, 2022, **23**, 7241.
6 D. Cirri, F. Bartoli, A. Pratesi, E. Baglini, E. Barresi and T. Marzo, *Biomedicines*, 2021, **9**, 504.
7 T. Gamberi and M. Hanif, *Biomedicines*, 2022, **10**, 2573.
8 M. G. Ferraro, M. Piccolo, G. Misso, R. Santamaria and C. Irace, *Pharmaceutics*, 2022, **14**, 954.
9 L. Todorov and I. Kostova, *Molecules*, 2023, **28**, 1959.
10 V. M. Miranda, *Rev. Inorg. Chem.*, 2022, **42**, 29–52.
11 R. T. Mertens, S. Gukathasan, A. S. Arojojoye, C. Olelewe and S. G. Awuah, *Chem. Rev.*, 2023, **123**, 6612–6667.
12 A. Balfourier, J. Kolosnjaj-Tabi, N. Luciani, F. Carn and F. Gazeau, *Proc. Natl. Acad. Sci. U. S. A.*, 2020, **117**, 22639–22648.
13 N. R. S. Sibuyi, K. L. Moabelo, A. O. Fadaka, S. Meyer, M. O. Onani, A. M. Madiehe and M. Meyer, *Nanoscale Res. Lett.*, 2021, **16**, 1–27.
14 K. Bromma and D. B. Chithrani, *Nanomaterials*, 2020, **10**, 1671.
15 Y. Lu, X. Ma, X. Chang, Z. Liang, L. Lv, M. Shan, Q. Lu, Z. Wen, R. Gust and W. Liu, *Chem. Soc. Rev.*, 2022, **51**, 5518–5556.
16 K.-C. Tong, D. Hu, P.-K. Wan, C.-N. Lok and C.-M. Che, *Front. Chem.*, 2020, **8**, 587207.
17 G. Moreno-Alcántar, P. Picchetti and A. Casini, *Angew. Chem.*, 2023, e202218000.
18 J. Jiang, X. Xiong and T. Zou, *Acc. Chem. Res.*, 2023, **56**, 1043–1056.
19 A. Giorgio and A. Merlino, *Coord. Chem. Rev.*, 2020, **407**, 213175.
20 A. Geri, L. Massai and L. Messori, *Molecules*, 2023, **28**, 5196.
21 R. P. Herrera and M. C. Gimeno, *Chem. Rev.*, 2021, **121**, 8311–8363.
22 L. Rocchigiani and M. Bochmann, *Chem. Rev.*, 2020, **121**, 8364–8451.
23 M. C. Gimeno, *Modern Supramolecular Gold Chemistry: Gole-Metal Interactions and Applications*, 2008, pp. 1–63.
24 P. Pyykkö, *Angew. Chem., Int. Ed.*, 2004, **43**, 4412–4456.
25 B. Đ. Glišić and M. I. Djuran, *Dalton Trans.*, 2014, **43**, 5950–5969.
26 S. Nobili, E. Mini, I. Landini, C. Gabbiani, A. Casini and L. Messori, *Med. Res. Rev.*, 2010, **30**, 550–580.
27 T. Zou, C. T. Lum, C.-N. Lok, J.-J. Zhang and C.-M. Che, *Chem. Soc. Rev.*, 2015, **44**, 8786–8801.
28 A. L. Noffke, A. Habtemariam, A. M. Pizarro and P. J. Sadler, *Chem. Commun.*, 2012, **48**, 5219–5246.
29 R. D. Hancock and A. E. Martell, *Chem. Rev.*, 1989, **89**, 1875–1914.
30 M. A. Carvajal, J. J. Novoa and S. Alvarez, *J. Am. Chem. Soc.*, 2004, **126**, 1465–1477.
31 K. H. Thompson and C. Orvig, *Dalton Trans.*, 2006, 761–764.
32 S. Gukathasan and S. G. Awuah, *EIBC*, 2022, 1–32.
33 A. S. Arojojoye, B. Walker, J. C. Dawahare, M. A. O. Afrifa, S. Parkin and S. G. Awuah, *ACS Appl. Mater. Interfaces*, 2023, **15**, 43607–43620.
34 A. S. Arojojoye and S. G. Awuah, *Coord. Chem. Rev.*, 2025, **522**, 216208.
35 A. G. Csákÿ and M. T. Molina, *Encyclopedia of reagents for organic synthesis*, 2001.
36 T. Hatakeyama, Y. Kondo, Y.-i. Fujiwara, H. Takaya, S. Ito, E. Nakamura and M. Nakamura, *Chem. Commun.*, 2009, 1216–1218.
37 H. Chea, H.-S. Sim and J. Yun, *Adv. Synth. Catal.*, 2009, **351**, 855–858.
38 K. Motokura, N. Takahashi, D. Kashiwame, S. Yamaguchi, A. Miyaji and T. Baba, *Catal. Sci. Technol.*, 2013, **3**, 2392–2396.
39 M. C. Neary, P. J. Quinlivan and G. Parkin, *Inorg. Chem.*, 2018, **57**, 374–391.
40 A. Tsuboyama, K. Kuge, M. Furugori, S. Okada, M. Hoshino and K. Ueno, *Inorg. Chem.*, 2007, **46**, 1992–2001.
41 Y. Yamazaki, T. Tsukuda, S. Furukawa, A. Dairiki, S. Sawamura and T. Tsubomura, *Inorg. Chem.*, 2020, **59**, 12375–12384.
42 H. R. Shahsavari, S. Chamyani, R. B. Aghakhanpour, V. Dolatyari and S. Paziresh, *New J. Chem.*, 2023, **47**, 1435–1443.
43 M. Osawa, I. Kawata, S. Igawa, M. Hoshino, T. Fukunaga and D. Hashizume, *Chem. – Eur. J.*, 2010, **16**, 12114–12126.
44 N. Mirzadeh, T. S. Reddy, S. H. Privér and S. K. Bhargava, *Dalton Trans.*, 2019, **48**, 5183–5192.
45 E. Bortolamiol, F. Fama, Z. Zhang, N. Demitri, L. Cavallo, I. Caligiuri, F. Rizzolio, T. Scattolin and F. Visentin, *Dalton Trans.*, 2022, **51**, 11135–11151.
46 H. R. Shahsavari, J. Hu, S. Chamyani, Y. Sakamaki, R. B. Aghakhanpour, C. Salmon, M. Fereidoonnezhad, A. Mojaddami, P. Peyvasteh and H. Beyzavi, *Organometallics*, 2020, **40**, 72–82.
47 A. S. Arojojoye, C. Olelewe, S. Gukathasan, J. H. Kim, H. Vekaria, S. Parkin, P. G. Sullivan and S. G. Awuah, *J. Med. Chem.*, 2023, **66**, 7869–7979.
48 D. Varna, D. I. Zainuddin, A. G. Hatzidimitriou, G. Psomas, A. A. Pantazaki, R. Papi, P. Angaridis and P. Aslanidis, *Mater. Sci. Eng., C*, 2019, **99**, 450–459.
49 E. K. Dennis, J. H. Kim, S. Parkin, S. G. Awuah and S. Garneau-Tsodikova, *J. Med. Chem.*, 2020, **63**, 2455–2469.
50 J. H. Kim, S. Ofori, S. Parkin, H. Vekaria, P. G. Sullivan and S. G. Awuah, *Chem. Sci.*, 2021, **12**, 7467–7479.
51 L. Wempe, R. Mohamed, J. Warinner, T. Goretsky, M. Avdiushko, J. Kim, A. Abomhya, G. Lee, S. Awuah, T. Barrett and N. Kapur, *Gastroenterology*, 2022, **162**, S2.
52 R. Mohamed, J. Warinner, L. Wempe, M. Avdiushko, T. Goretsky, J. Kim, A. Abomhya, G. Lee, S. Awuah, T. Barrett and N. Kapur, *Gastroenterology*, 2022, **162**, S2–S3.
53 M. Osawa, I. Kawata, S. Igawa, A. Tsuboyama, D. Hashizume and M. Hoshino, *Eur. JIC*, 2009, (25), 3708–3711.

54 A. V. Kalvelytė, A. Imbrasaitė, N. Krestnikova and A. Stulpinas, in *Advances in molecular toxicology*, Elsevier, 2017, vol. 11, pp. 123–202.
55 J. Deng, Y. Gou, W. Chen, X. Fu and H. Deng, *Bioorg. Med. Chem.*, 2016, **24**, 2190–2198.
56 C. D. Sanghvi, P. M. Olsen, C. Elix, S. B. Peng, D. Wang, D. M. Shin, K. I. Hardcastle, C. E. MacBeth and J. F. Eichler, *J. Inorg. Biochem.*, 2013, **128**, 68–76.
57 P. M. Olsen, C. Ruiz, D. Lussier, B. K. Le, N. Angel, M. Smith, C. B. Hwang, R. Khatib, J. Jenkins and K. Adams, *J. Inorg. Biochem.*, 2014, **141**, 121–131.
58 R. Charlton, C. Harris, H. Patil and N. Stephenson, *Inorg. Nucl. Chem. Lett.*, 1966, **2**, 409–414.
59 K. J. Kilpin, W. Henderson and B. K. Nicholson, *Inorg. Chim. Acta*, 2009, **362**, 5080–5084.
60 A. Abedi, M. Zare Dehnavi, N. Safari and V. Amani, *Synth. React. Inorg., Met.-Org., Nano-Met. Chem.*, 2015, **45**, 133–138.